Computational and Structural Biotechnology Journal 18 (2020) 3977–3986

COMPUTATIONAL AND STRUCTURAL BIOTECHNOLOGY JOURNAL

journal homepage: www.elsevier.com/locate/csbj

Genetic perturbation of IFN-α transcriptional modulators in human endothelial cells uncovers pivotal regulators of angiogenesis

Francesco Ciccarese [a,1], Angela Grassi [a,1], Lorenza Pasqualini [a,2], Stefania Rosano [b], Alessio Noghero [b,3], Francesca Montenegro [c], Federico Bussolino [b,d], Barbara Di Camillo [e,f], Lorenzo Finesso [g], Gianna Maria Toffolo [e], Stefania Mitola [h], Stefano Indraccolo [a,*]

[a] Immunology and Molecular Oncology Unit, Veneto Institute of Oncology IOV – IRCCS, via Gattamelata 64, 35128 Padova, Italy
[b] Candiolo Cancer Institute - IRCCS, Strada Provinciale 142, km 3.95, 10060 Candiolo, Italy
[c] Department of Surgery, Oncology and Gastroenterology, University of Padova, via Gattamelata 64, 35128 Padova, Italy
[d] Department of Oncology, University of Torino Medical School, via Verdi 8, 10124 Torino, Italy
[e] Department of Information Engineering, University of Padova, via Gradenigo 6, 35131 Padova, Italy
[f] CRIBI Innovative Biotechnology Center, University of Padova, viale Colombo 3, 35131 Padova, Italy
[g] Institute of Electronics, Computer and Telecommunication Engineering, CNR, corso Stati Uniti 4, 35127 Padova, Italy
[h] Department of Molecular and Translational Medicine, University of Brescia, viale Europa 11, 25123 Brescia, Italy

ARTICLE INFO

Article history:
Received 22 July 2020
Received in revised form 24 November 2020
Accepted 24 November 2020
Available online 2 December 2020

Keywords:
IFN-α
Transcriptional modulators
Regulatory network
CXCL10
Angiogenesis

ABSTRACT

Interferon-α (IFN-α) comprises a family of 13 cytokines involved in the modulation of antiviral, immune, and anticancer responses by orchestrating a complex transcriptional network. The activation of IFN-α signaling pathway in endothelial cells results in decreased proliferation and migration, ultimately leading to suppression of angiogenesis. In this study, we knocked-down the expression of seven established or candidate modulators of IFN-α response in endothelial cells to reconstruct a gene regulatory network and to investigate the antiangiogenic activity of IFN-α. This genetic perturbation approach, along with the analysis of interferon-induced gene expression dynamics, highlighted a complex and highly interconnected network, in which the angiostatic chemokine C-X-C Motif Chemokine Ligand 10 (CXCL10) was a central node targeted by multiple modulators. IFN-α-induced secretion of CXCL10 protein by endothelial cells was blunted by the silencing of Signal Transducer and Activator of Transcription 1 (STAT1) and of Interferon Regulatory Factor 1 (IRF1) and it was exacerbated by the silencing of Ubiquitin Specific Peptidase 18 (USP18). *In vitro* sprouting assay, which mimics *in vivo* angiogenesis, confirmed STAT1 as a positive modulator and USP18 as a negative modulator of IFN-α-mediated sprouting suppression. Our data reveal an unprecedented physiological regulation of angiogenesis in endothelial cells through a tonic IFN-α signaling, whose enhancement could represent a viable strategy to suppress tumor neoangiogenesis.

1. Introduction

Interferon-α (IFN-α) are a family of cytokines endowed with antiviral, immunomodulatory and anticancer activities, secreted by various cell types in response to pathogens, cancer cells or during immune responses [1–5]. IFN-α production is triggered by recognition of pathogens – and presumably dying cancer cells [6] – by Toll-like receptors (TLRs), through NF-κB signaling and recruitment of transcription factors of the Interferon Regulatory Factor (IRF) family [7]. Upon ligand binding, IFN receptors activate the Janus Kinase (JAK) – Signal Transducer and Activator of Transcription (STAT) pathway, along with MAPK, PI3K and AKT pathways [8–11]. Rapid phosphorylation of TYK2 and JAK1 is

* Corresponding author.
E-mail addresses: francesco.ciccarese@iov.veneto.it (F. Ciccarese), angela.grassi@unipd.it (A. Grassi), pasqualini.lorenza@gmail.com (L. Pasqualini), stefania.rosano@ircc.it (S. Rosano), anoghero@lrri.org (A. Noghero), francesca.montenegro@phd.unipd.it (F. Montenegro), federico.bussolino@unito.it (F. Bussolino), barbara.dicamillo@unipd.it (B. Di Camillo), lorenzo.finesso@ieiit.cnr.it (L. Finesso), giannamaria.toffolo@unipd.it (G.M. Toffolo), stefania.mitola@unibs.it (S. Mitola), stefano.indraccolo@unipd.it (S. Indraccolo).

[1] These Authors share first co-authorship.
[2] Present address: Diagnostics and Genomics Group, Agilent Technologies Inc., Santa Clara, CA, USA.
[3] Present address: Lovelace Biomedical Research Institute, 2425 Ridgecrest Dr. SE, Albuquerque, NM 87108-5127, USA.

https://doi.org/10.1016/j.csbj.2020.11.048

followed by phosphorylation of STAT1 and STAT2, which interact with IRF9, forming a complex known as ISGF3. This complex migrates to the nucleus and binds to IFN-stimulated response elements (ISREs), thus leading to transcription of >2000 IFN-stimulated genes (ISGs) [12].

In the context of cancer, besides directly impinging on cancer cell proliferation and promoting adaptive immune response, IFN-α mediates antitumor effects through inhibition of angiogenesis [13]. IFN-α antiangiogenic activity relies on reducing the secretion of proangiogenic factors – such as vascular endothelial growth factor (VEGF) [14] or interleukin-8 (IL-8) [15] – and promoting release of antiangiogenic factors – such as the angiostatic chemokines C-X-C Motif Chemokine Ligand (CXCL) 9 and 10 [16,17] – by cancer and stromal cells. This imbalance between pro- and antiangiogenic factors in an IFN-α rich microenvironment contrasts proliferation of endothelial cells (EC) and formation of new blood vessels. Indeed, treatment with IFN-α is associated with reduced microvessel density and increased coverage of blood vessels by pericytes [18,19], a marker of vascular normalization. IFN-α inhibits angiogenesis also by direct effects on EC proliferation and migration [20–22], and by inducing replicative senescence following chronic exposure [23]. Notably, genetic alterations in cancer cells or certain features of the tumor microenvironment dampen IFN signaling [24,25]. In this respect, high concentrations of VEGF – which are typically found in the hypoxic tumor microenvironment – counteract antiangiogenic activity of IFN-α, as VEGF signaling leads to IFN-α Receptor Subunit 1 (IFNAR1) degradation [26] and blockade of IFN signaling in EC. These vulnerabilities, along with marked side effects, likely account for the limited success of systemic IFN-α administration in the clinic.

The complex biological effects of IFN-α on angiogenesis are empowered by strong IFN-induced transcriptional responses in EC, which comprise both an amplification component as well as negative feedback control. Although several studies, including ours, previously investigated the static IFN signature in EC and identified a core of genes modulated by IFN-α [22,27,28], there is still limited knowledge about temporal expression profiles induced by IFN-α. Aim of this study was to reconstruct the regulatory network of the IFN-α transcriptional response in EC by analyzing the dynamic behavior of several ISGs and by investigating how perturbation of certain IFN-α transcriptional modulators impacts on the IFN signature and on angiogenesis.

2. Materials and methods

2.1. Cells and reagents

Human umbilical vein endothelial cells (HUVECs) were isolated at University of Brescia and at University of Torino Medical School from healthy informed volunteers. Additional HUVECs were kindly provided by Dr. Giampietro Viola (Department of Woman and Children Health, University of Padova, Italy) and Dr. Roberto Ronca (Department of Molecular and Translational Medicine, University of Brescia, Italy). For routine culture, cells were maintained at 37°C in a humidified 5% CO_2 atmosphere in M200 medium supplemented with Low-Serum Growth Supplement (LSGS; Life Technologies, Paisley, UK) and antibiotics (100 U/mL streptomycin and 100 U/mL penicillin; Sigma-Aldrich, Saint Louis, MO, USA). Cells were stimulated with human recombinant IFN-α2 (Merck & Co., White House Station, NJ, USA) using a final concentration of 1,000 U/ml. This concentration was chosen based on our previous studies [22,29]. Where indicated, HUVECs were treated with the JAK inhibitor ruxolitinib (2 μM, Selleckchem, Munich, Germany). Each biological replicate was obtained by a pool of 4 donors and all experiments were conducted between passage 2 and 7 at a confluence of 70–80%.

2.2. Time-course IFN-α stimulation

HUVECs ($3.5x10^5$ per well) were seeded onto 35 mm tissue culture-treated Petri dishes and cultured as described above. The day of the experiment, 2 ml of fresh medium, in absence or presence of 1,000 UI/ml IFN-α, was added to each well. Time-course data were collected at nine time points (0, 1, 2, 4, 6, 8, 10, 12 and 24 h) with double stimulation: IFN-α stimulation at 0 h and wash-out at 8 h. Silencing data, obtained by knocking-down candidate IFN-α modulators, were collected in a short time series of four points (0 h, 2 h, 8 h, 12 h) with double stimulation as before. The two sampling protocols for the collection of time-course and silencing data are shown in Fig. S1, Supplementary data 1. All experiments were carried out in biological duplicates.

2.3. siRNA-mediated gene silencing

HUVECs ($3.5x10^5$ per well) were seeded onto 6-well plates and maintained in standard culture conditions. After 24 h, cells were transfected with Stealth siRNAs (Life Technologies) for RNAi-mediated silencing of seven candidate IFN-α modulators (STAT1, IFIH1, IRF1, IRF7, GBP1, OAS2 and USP18) using Lipofectamine RNAiMAX Transfection Reagent (Life Technologies). For each target gene, a set of three siRNAs (Supplementary Table A1, Supplementary file 1) was tested for RNAi activity and the Stealth siRNA showing the highest level of knockdown (>75%) was selected to be used for subsequent experiments. A negative control with low GC content (Life Technologies) was also included in the experimental design as internal calibrator (siCTRL). In detail, each siRNA was diluted in 500 μl Opti-MEM® I with GlutaMAX™-I transfection medium (Life Technologies) with 4 μl Lipofectamine RNAiMAX Transfection Reagent and added to 1.5 ml culture medium, to obtain 10 nM final concentration. Transfection was blocked 6 h post-siRNA administration by replacing the transfection medium with fresh culture medium. Upon 48 h transfection, 24 h IFN-α stimulation was carried out for subsequent measurement of CXCL10 protein through ELISA analysis or for RNA isolation according to the time-course.

2.4. RNA isolation and cDNA synthesis

Total RNA was extracted using TRIzol Reagent (Life Technologies) according to the manufacturer's instructions. RNA quality and quantity were checked by measurement of absorbance at 230 nm, 260 nm, and 280 nm by means of nanospectrophotometric analysis. Total RNA (1–2 μg) was reverse transcribed using High Capacity RNA-to-cDNA Kit (Life Technologies), according to manufacturer's instructions.

2.5. Measurement of gene expression using quantitative RT-PCR

Gene expression was assessed by SYBR® Green qRT-PCR analysis using primers (purchased from Sigma-Aldrich) listed in Supplementary Table A2 (Supplementary file 1). qRT-PCR reactions were performed for 45 cycles using a Light Cycler 480 II thermal cycler (Roche, Basel, Switzerland). mRNA expression levels were calculated using the $2^{-\Delta\Delta Ct}$ method and *LMNA* as reference gene. PCR reactions were performed in duplicate.

2.6. TaqMan Array Cards analysis

A panel of 96 pre-selected genes (Supplementary Table A3, Supplementary file 1), related to IFN-α transcriptional response, was

screened by Custom TaqMan Array Cards (Life Technologies, format 96b), using TaqMan Universal PCR Master Mix (Life Technologies), to obtain both the time-course and the perturbation data. The criteria used for the pre-selection of transcripts were described in our previous work, Grassi *et al.* [29]. qRT-PCR reactions were run on an ABI Prism 7900HT Sequence Detection System (Life Technologies) and raw data were extracted using the SDS v2.4 software package (Life Technologies). *LMNA* was chosen as reference gene for the time-course expression data, being the most stable gene in this dataset. *JAK1* was the most stable gene across the different silencing experiments and it was taken as reference gene for the normalization of qRT-PCR perturbation data.

2.7. Time-course data analysis: K-means clustering

In order to identify the main temporal expression patterns characterizing IFN-α transcriptional response, $-\Delta Ct$ temporal profiles of the monitored genes were clustered using the K-means algorithm. The number of clusters K was set to 5 and the measure of similarity adopted was the Pearson correlation. The clustering algorithm was applied to 87 transcripts, excluding from the analysis the candidate housekeeping (*18S*, *HMBS* and *LMNA*) and six other genes with incomplete $-\Delta Ct$ profiles.

2.8. Perturbation data analysis: Significant regulations and network reconstruction

The effects of each siRNA were evaluated with respect to a calibrator siRNA using the comparative threshold cycle method ($\Delta\Delta Ct$ method). The significance analysis, developed to elicit significant regulations induced by each perturbation, and the inference method, used to reconstruct a regulatory subnetwork, were originally described in [29]. Briefly, for the significance analysis we proposed a two-stage selection procedure that first filters observations based on the $\Delta\Delta Ct$ variance distribution, and then performs a variable-by-variable statistical test procedure, which uses the biological variance estimated through a measurement error model, to assign a p-value to each modulation. A Bonferroni multiple testing correction was applied to control the false positive rate (FPR) in the gene callings at 5%. All the analyses were performed in the R statistical environment. The adopted sampling scheme allowed to distinguish between modulators exerting their action in the early (2 h) and/or late (8 h) IFN-α activation phase and in the phase of IFN-α removal (12 h). Significant regulations, induced by the silencing of the seven IFN-α modulators, were graphically represented as edges of a transcriptional influence network. If, by knocking down a modulator, another gene was significantly down-regulated (or up-regulated) during the IFN-α stimulation phase, the corresponding regulation was interpreted as an activation (or repression) relationship, from the silenced gene to its target. Regulations occurring in the IFN-α removal phase were depicted as dotted lines, without specifying the type of regulation. If a gene was significantly modulated during both stimulation and wash-out phase, only the regulation in the stimulation phase was reported in the reconstructed network. We refer to [29] for the complete description of the inference method to reconstruct putative multi-output feed-forward loop (FFL) subnetworks.

2.9. Measurement of CXCL10 levels

HUVECs were transfected with STAT1-, IFIH1-, USP18- and IRF1-specific siRNA and treated with IFN-α as described above. Cell pellets as well as supernatant were collected and stored at −80°C until further use. The amount of CXCL10 protein in cell supernatants was measured by ELISA (KAC2361, Thermo Fisher, Waltham, MA, USA) in clear flat-bottomed 96-well plates according to the manufacturer's instructions. Prior to analysis, collected supernatant was thawed on ice and centrifuged at 4°C for 10 min at 14,000 rpm to remove cell debris.

2.10. Measurement of IFN-α levels

HUVECs (3.5×10^5 per well) were seeded onto 6-well plates and maintained in standard culture conditions. Supernatants were collected 30 h after culture medium change, centrifuged at 4°C for 20 min at 1,000 g to remove insoluble impurities and cell debris, and stored at −80°C until further use. The amount of IFN-α protein in cell supernatants was measured by ELISA (EH3252, Fine Biotech, Wuhan, China) in clear flat-bottom 96-well plates according to the manufacturer's instructions. Cell lysates were collected for further western blot analysis.

2.11. Western blot analysis

Cell lysates were prepared in RIPA lysis buffer (Cell Signaling Technology, Danvers, MA, USA) containing protease and phosphatase inhibitor cocktails (Sigma-Aldrich). Proteins were quantified using Quantum Micro protein Assay (EuroClone, Milan, Italy) and loaded in a midi polyacrylamide gel 4–12% (Life Technologies). Separated proteins were transferred for 2 h at 400 mA on a nitrocellulose membrane (GE Healthcare, Glattbrugg, Switzerland). Immunoprobing was performed overnight at 4°C with the following primary antibodies: STAT-1, polyclonal Ab, 1:1000 (Thermo Fisher Scientific Inc., Waltham, MA, USA), p-STAT-1 (Tyr701) (58D6), 1:1000 (Cell Signaling Technology), α-tubulin, 1:4000 (Sigma-Aldrich), followed by hybridization with horseradish peroxidase-conjugated anti-rabbit or anti-mouse Ab (Perkin Elmer, Waltham, MA, USA). Immunoreactive bands were detected by chemiluminescence using Western Lightning Plus ECL reagents (Perkin Elmer) and a digital imager (Alliance LD2, UVITEC, Cambridge, UK). α-tubulin was used to assess protein expression.

2.12. Spheroid capillary sprouting assay

EC spheroids were generated as previously described [30], with minor modifications. HUVECs within third passage were trypsinized and cultured in hanging drops (800 cells/drop) in M199 containing 10% FBS and 0.4% (w/v) methylcellulose. After 20 h or overnight incubation, spheroids were collected and embedded in a solution containing 15% FBS, 0.5% (w/v) methylcellulose, 1 mg/ml rat tail collagen solution (Sigma-Aldrich), 30 mM HEPES and M199 from 10X concentrate. 0.1 M NaOH was added to adjust the pH to 7.4 to induce collagen polymerization. Sprouting was induced by addition of 20 ng/ml recombinant human VEGF-A (R&D Systems, Minneapolis, MN, USA) to the collagen solution. When indicated, IFN-α (600 UI/ml) was added to the hanging drop culture, and to the collagen solution. Spheroids were imaged after 18 h incubation at 37°C in a 5% CO_2 incubator. Image analysis was performed with ImageJ software (National Institutes of Health, Bethesda, MD, USA; RRID:SCR_003070).

2.13. Statistical analysis

Results are expressed as mean value ± standard error. The non-parametric Mann-Whitney test was chosen to assess the statistical significance of differential gene expression between gene specific-siRNA sample and the internal calibrator, indicated as fold change, as well as differences in CXCL10 secretion and sprout areas. Differences were considered statistically significant when $p < 0.05$.

3. Results

3.1. Transcriptional expression patterns induced by IFN-α in EC

We first analyzed the dynamic expression profiles of 87 ISGs in IFN-α-treated HUVECs. Five main temporal patterns of modulations were identified in response to IFN-α stimulation (time point 0 h) and subsequent wash-out (time point 8 h) by K-means clustering (Fig. 1). Clusters 1, 3, and 5 show three strong patterns of up-regulation, with the majority of genes belonging to the top signature of IFN-α at 5 h [22]. Cluster 2 displays a profile of activation/deactivation with a plateau phase from 2 h to 10 h, interestingly *JAK1* and *STAT1* fall in it. Finally, cluster 4 is characterized by a fluctuating expression profile with several peaks, and includes *IFNAR1*, *IFNAR2*, and *TYK2*. Complete results, with the list of genes belonging to each cluster, are presented in Table 1.

3.2. Key modulators of IFN-α signature in EC

RNAi-mediated knockdown of seven established (IRF1, IRF7, STAT1, USP18) or candidate (GBP1, OAS2, IFIH1) IFN-α modulators [29,31–34] was achieved using Stealth siRNAs and a panel of core IFN-α regulated genes was monitored by TaqMan Array Cards (see Materials and Methods). Statistical analysis showed STAT1 and IFIH1 as mainly positive regulators, and USP18, GBP1 and IRF1 as mainly negative regulators of IFN-α transcriptional response. In contrast, IRF7 and OAS2 acted equally in both directions. STAT1 was confirmed as the primary positive transcriptional modulator of IFN-α; following its silencing several genes were significantly down-regulated and only few genes up-regulated. Conversely, USP18 was the strongest negative transcriptional modulator and its silencing caused a massive up-regulation of genes, including some involved in cell-to-cell adhesion. Table 2 summarizes the overall impact, together with the specific effects in the IFN-α activation and deactivation phase, of the seven modulators on the panel of genes monitored by qRT-PCR. Detailed results of the significance analysis are shown in Supplementary Tables A4–A10 (Supplementary file 1). Noteworthy, among the strongest IFN-α modulators, USP18, GBP1 and IFIH1 are non-transcription factors (TFs).

3.3. IFN-α controls a complex transcriptional network in EC

Drawing on the significant results of perturbation data analysis, a complex network of influence relationships was reconstructed (Supplementary file 2). USP18 emerged as a potent negative regulator of IFN-α, exerting its action by inhibiting several genes, among which members of the RIG-I-like receptor (RLR) family

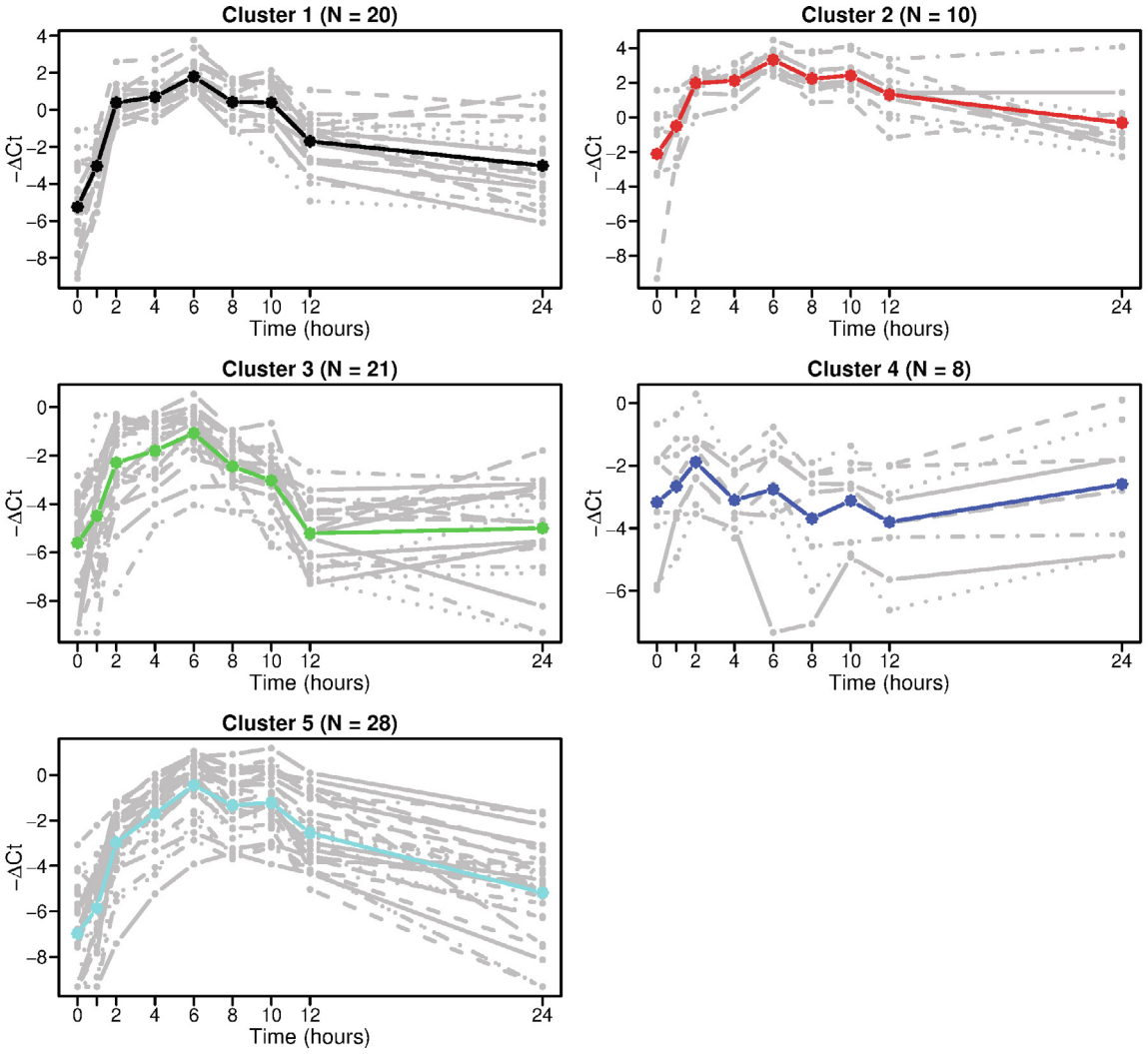

Fig. 1. K-means clustering of $-\Delta Ct$ temporal profiles. Five temporal patterns of modulations were identified in response to IFN-α stimulation (0 h) and subsequent wash-out (8 h). Single gene profiles are depicted in gray, while cluster average profiles are colored. N indicates the cluster size.

Table 1
Results of K-means clustering.

Detailed list of genes in each cluster
Cluster 1 (N = 20)
APOL6; BST2; DDX58; IFI6; IFIH1; IFIT1; IFIT2; IFIT3; IFITM1; OAS1; OAS2; PLSCR1; PML; RSAD2; RTP4; SAMHD1; SHFL; SP110; STAT2; USP18.
Cluster 2 (N = 10)
CXCL11; ELF1; GBP1; IFI27; ISG20; JAK1; MX1; STAT1; TAP1; UBE2L6.
Cluster 3 (N = 21)
APOL2; BLZF1; CFB,C2; DHX58; DSP; GCH1; IDO1; IFI16; IFIT5; IL15RA; IRF1; IRF9; PSMB8; SAMD9; SLC25A28; TDRD7; TENT5A; THEMIS2; TMEM140; TRIM21; ZC3HAV1.
Cluster 4 (N = 8)
ATF3; BNIP3; IFNAR1; IFNAR2; IRF3; TP53; TYK2; VEGFA.
Cluster 5 (N = 28)
APOL1; APOL3; CASP1; CXCL10; DDX60; GMPR; HERC5; HERC6; IFI30; IFI35; IFI44; IFI44L; IRF7; LGALS9; MX2; OAS3; OASL; PLEKHA4; PSMB9; RARRES3; SECTM1; SLC15A3; TAP2; TLR3; TNFSF10; TRANK1; TRIM14; XAF1.

Table 2
Number of genes down- and up-regulated upon silencing of IFN-α modulators.

Silencing	IFN-α activation phase		IFN-α deactivation phase		Overall impact	
	Down	Up	Down	Up	Down	Up
STAT1	17	4	0	0	17	4
IFIH1	8	3	1	0	9	3
OAS2	5	5	2	0	7	5
IRF7	2	1	1	5	3	6
IRF1	2	6	0	4	2	10
GBP1	1	9	2	10	3	19
USP18	0	46	0	7	0	53

(i.e. *DDX58*, *IFIH1*, *DHX58*, encoding for RIG-I, MDA5 and LGP2, respectively). The fine regulation of antiviral immune response, implemented by the complex transcriptional network activated by IFN-α, is achieved through the regulation not only of cytosolic RNA sensors (RIG-I, MDA5 and LGP2) but also of endosomal RNA receptors, e.g. TLR3. Indeed, *TLR3* gene appeared to be negatively regulated during IFN-α activation phase by both IRF1 and OAS2. Moreover, IFN-α activation induced the expression of many intrinsic antiviral restriction factors capable of blocking the virus replication cycle at different stages (IFITM1, uncoating; TRIM21, replication of antibody-opsonized viruses; APOBEC3G and SAMHD1, replication; viperin, encoded by *RSAD2*, assembly). The inferred influence network contains a lot of information that may be useful to unveil the mechanisms underlying the different activities accomplished by IFN-α. In order to distill information worth of biological validation we applied the method developed in [29] to extract putative feed-forward loop (FFL) circuits from perturbation data. We thus reconstructed a multiple-output FFL regulatory subnetwork in which *STAT1*, *IFIH1*, *IRF1*, *IRF7*, *GBP1*, *OAS2*, and *USP18* are the only regulators (Fig. 2). This representation is more effective in highlighting the action of multiple modulators on the same targets. Interestingly, three genes seem to play the role of "IFN-α-sentinels", being modulated by all the seven perturbations (*SAMD9*), by 6 perturbations out of 7 (*CXCL10*), and by 5 (*TENT5A*). Moreover, cell response to IFN-α appears regulated through negative feedback control, which acts both at the level of the two receptor subunits and at the level of endogenous IFN production.

3.4. STAT1, USP18 and IRF1 modulate CXCL10 levels in EC following IFN-α stimulation

To validate the transcriptional regulations inferred in our multiple-output FFL regulatory subnetwork (Fig. 2), we measured CXCL10 protein levels in tissue culture media conditioned by STAT1-, USP18-, IFIH1- and IRF1-silenced HUVECs, compared to HUVECs transfected with a scrambled siRNA (siCTRL). CXCL10 is an antiangiogenic chemokine known to be induced by type I IFNs and can be accurately measured in supernatants by ELISA. Following siRNA transfection, analysis by qRT-PCR disclosed marked reduction (>60%) of relevant transcript levels in all cases analyzed (Fig. S2, Supplementary file 1). As expected, IFN-α treatment increased secretion of CXCL10 in HUVECs transfected with the control siRNA (siCTRL) (Fig. 3). Moreover, STAT1 and IRF1 silencing significantly reduced IFN-α-induced secretion of CXCL10 protein. In contrast, IFIH1 silencing was associated with minor variations in CXCL10 levels. Finally, CXCL10 secretion increased over 30-fold following IFN-α treatment in USP18-silenced HUVECs (Fig. 3).

3.5. Modulation of signaling downstream IFN-α affects in vitro sprouting of EC

The involvement of the modulators identified by our transcriptional analysis in regulating antiangiogenic effect of IFN-α was validated using a spheroid capillary assay, which mimics sprouting angiogenesis *in vitro* [35]. Spheroids generated with HUVECs in which the expression of STAT1, USP18, IFIH1, GBP1 or IRF1 was knocked-down by specific siRNA, and spheroids generated with HUVECs transfected with a scrambled siRNA (siCTRL), were subjected to the sprouting assay, where VEGF-A was used as angiogenic stimulus, in the absence or in the presence of IFN-α (Fig. 4a). Quantification of sprout areas showed a marked reduction in sprouting activity when siCTRL cells were treated with IFN-α, thus indicating that in this model IFN-α is an effective inhibitor of angiogenesis (Fig. 4b). Silencing of STAT1 had a strong positive effect on sprouting and counteracted the inhibitory effect of IFN-α. The other interactors (USP18, IFIH1, GBP1, and IRF1) all demonstrated to act as sprouting inhibitors in the absence of IFN-α. While IFIH1 silencing did not show noticeable alterations compared to siCTRL upon addition of IFN-α, IRF1, GBP1 and USP18 silencing showed a diversified effect (Fig. 4b). In fact, both IRF1 and GBP1 silencing completely abrogated the inhibitory effect of IFN-α, resulting in spheroids with a sprout area comparable with that of spheroids not stimulated with IFN-α. This observation confirms the role of IRF1 as positive regulator of IFN-α signaling. On the con-

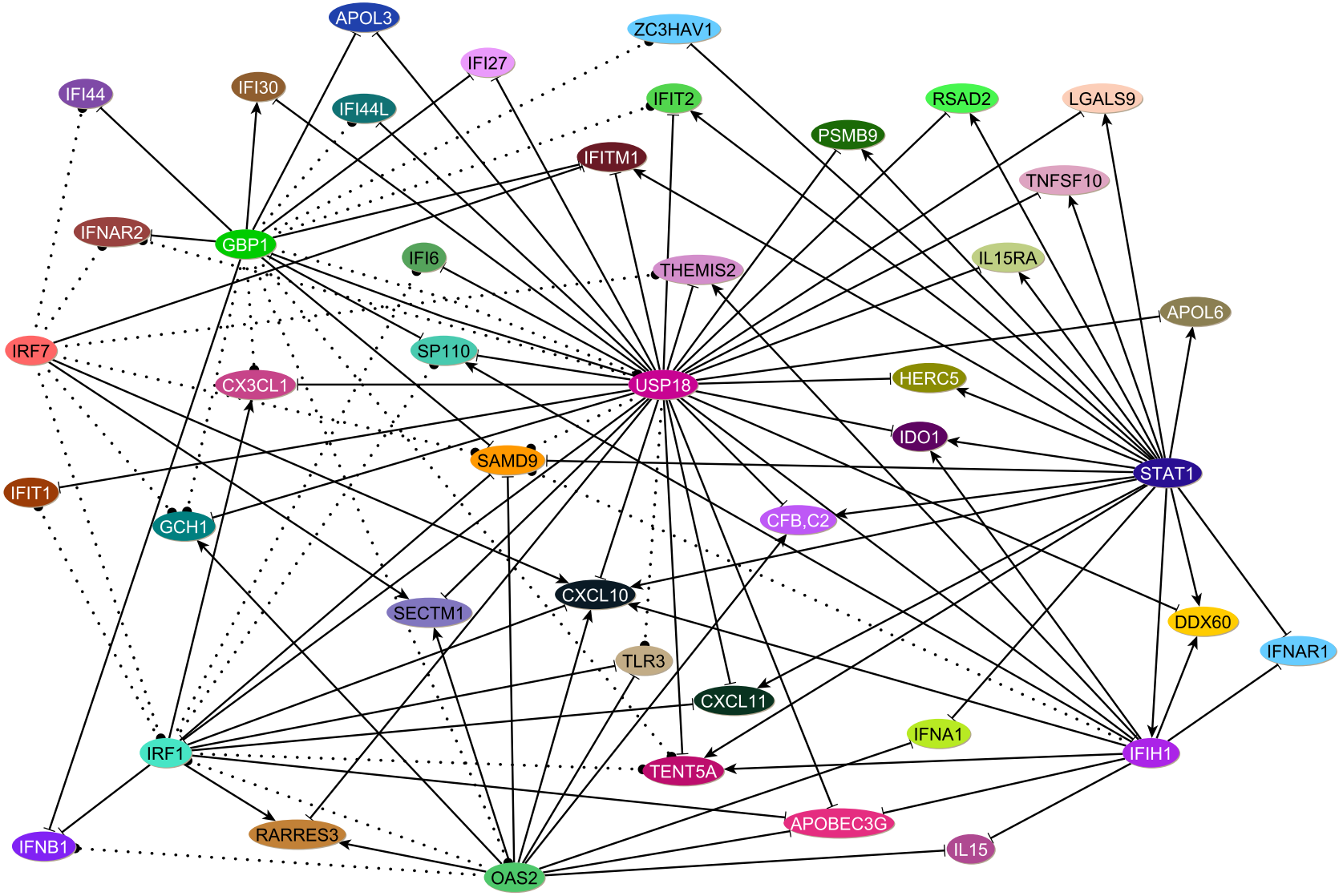

Fig. 2. IFN-α regulatory network inference. Multiple-output FFL regulatory subnetwork reconstructed from the silencing of the seven IFN-α modulators. Lines represent influence regulations in the IFN-α stimulation (2 h/8 h; solid line) and wash-out (12 h; dashed lines) phase. Arrow styles stand for: arrow, activation; ⊣, repression; dot, unspecified sign of regulation.

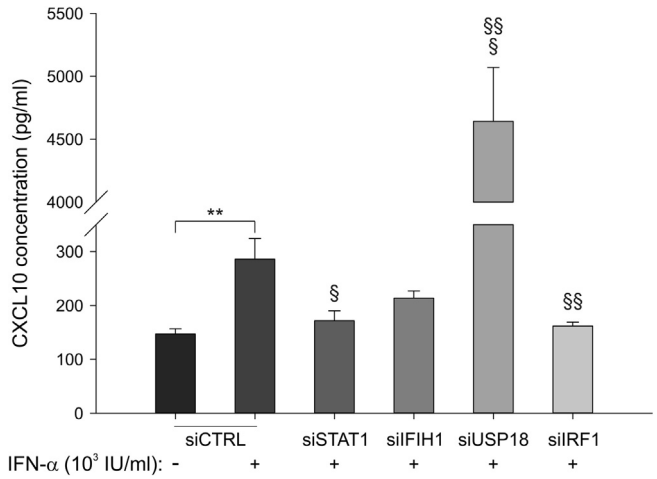

Fig. 3. Measurement of CXCL10 levels in supernatants of HUVECs following silencing of STAT1, IFIH1, USP18 and IRF1. Measurement of CXCL10 levels following STAT1, IFIH1, USP18 and IRF1 siRNA-mediated silencing in HUVECs from 3 different donors. ** p<0.01 siCTRL vs. siCTRL + IFN-α; § p<0.05, §§ p<0.01, §§§ p<0.001 siSTAT1/IFIH1/USP18/IRF1 + IFN-α vs. siCTRL + IFN-α.

trary, USP18 silencing reinforced the IFN-α-induced sprouting inhibition, thus supporting its role as negative regulator.

3.6. EC self-regulate their sprouting capacity by secreting endogenous IFN-α

The proangiogenic effect of STAT1 silencing, as well as the antiangiogenic effect of USP18 knock-down, in the absence of IFN-α suggest that a putative tonic IFN-α signaling could be physiologically active in EC. To test this possibility, we measured IFN-α protein levels in tissue culture medium conditioned by non-transfected HUVECs. Interestingly, small amounts of endogenous IFN-α (up to 91.57 pg/ml) were secreted by different pools of EC in the absence of genetic perturbation. Western blot analysis revealed that STAT1 is slightly phosphorylated in untreated EC, supporting the hypothesis that a physiological, tonic IFN-α signaling is active in these cells (Fig. S3, Supplementary file 1).

4. Discussion

Although over 60 years have passed since the discovery of IFN-α, it is still poorly understood how this potent cytokine controls its complex transcriptional network. Understanding the complex IFN-α response and its dynamics could provide putative novel targets of pharmacological intervention to modulate the pleiotropic activities of this cytokine. In this study, we analyzed the dynamic expression profiles of a subset of ISGs, known to be induced by IFN-α in EC [22], to reconstruct a gene regulatory network through the genetic perturbation of seven established or candidate modulators of IFN-α response.

The analysis of temporal profiles revealed that most of the ISGs in EC are rapidly up-regulated within 2 h following IFN-α treatment, including the selected IFN-α modulators (Table 1 and Fig. 1). These results are consistent with the observations of Mostafavi and colleagues in B-cells, where the response to IFN-α is even faster [36]. Interestingly, our analysis revealed that most of the genes involved in the activation of IFN-α signaling cascade belong to cluster 2 and cluster 4 (Table 1). STAT1 and JAK1 fall into cluster 2, which is characterized by a plateau phase from 2 h to 10 h. The fluctuating profile of cluster 4, which comprises type I IFN receptors and the signal transducer *TYK2*, highlights the complex temporal regulation of EC responsiveness to IFN-α.

Next, we generated perturbation data and applied the computational approach originally presented in our previous work [29] to elicit significant regulations and infer a transcriptional influence network controlled by IFN-α in EC. In [29], our theoretical method for the processing of perturbation data was exemplified on a case study to reconstruct an IFN-α regulatory module, in which STAT1 and IFIH1 were the only regulators. Here, we have extended the analysis to seven established or putative modulators of IFN-α signaling, showing how regulatory modules merge together in a highly interconnected influence network, which is useful to generate new hypotheses on the mechanism of action of the involved genes. The full results of significance analysis depicted a complex transcriptional network with 141 links (Supplementary file 2). As expected, we found STAT1 as the main positive regulator of IFN-α pathway. Moreover, our analysis revealed that IFN-α response is strongly counteracted by the isopeptidase USP18, which is among the genes most rapidly activated by this cytokine. This observation, along with the downregulation of IFNAR1 by STAT1, which we already described in [29], highlights that IFN-α pathway is finely regulated by negative feedback loops. USP18 is a well-established negative regulator of IFN-α signaling [37], which sustains JAK/STAT activation [38], thus exacerbating cell sensitivity to IFN-α. From our transcriptional analysis, it emerges that USP18 negatively regulates a much higher number of genes than those regulated by STAT1 (53 vs. 21) as well as the magnitude of CXCL10 protein modulation achieved following its perturbation is augmented (Fig. 3). Strikingly, in our model we identified two additional non-TFs, IFIH1 and GBP1, as key modulators of IFN-α transcriptional network. IFIH1 is a helicase involved in the recognition of double-stranded RNA viruses, as well both positive and negative stranded RNA viruses [39]. Upon activation, IFIH1 promotes the phosphorylation and nuclear transport of IRF3 and IRF7 by activating NF-κB pathway, thus leading to production of IFN-α and IFN-β [40]. Our data suggest that IFIH1 modulates IFN-α pathway even in the absence of viral RNA. The mechanism through which IFIH1 modulates IFN-α signaling regardless of pathogen recognition pathway deserves further investigation. This could imply a tonic IFN-α signaling through an autocrine loop and could have important implications in autoimmune diseases linked to IFIH1 polymorphisms, such as type 1 diabetes [41]. GBP1 is a GTPase involved in the regulation of a variety of cell functions, including inhibition of cell proliferation, immunity, endosomal trafficking, and autophagy [42]. Interestingly, Forster and colleagues observed that GBP1 binds to several regulatory cytoskeletal proteins, thus restraining T-cell receptor (TCR) signaling [43]. It is reasonable that GBP1 could limit IFN-α signaling as well, consistently with its role as negative IFN-α transcriptional modulator in EC and with the inferred negative regulation of GBP1 on IFNAR2, resulting by our analysis. Further studies are needed to assess whether the transcriptional network inferred by our computational approach is endothelial cell-specific or conserved among different types of cells, such as cancer cells or cells of the tumor microenvironment.

In the reconstructed influence network three nodes, namely *CXCL10*, *TENT5A*, and *SAMD9*, emerged as "IFN-α-sentinel genes" because significantly regulated following the silencing of at least 5 IFN-α transcriptional modulators. Among them CXCL10 is a potent angiostatic chemokine [44]. In EC, CXCL10 is a rapidly upregulated ISG, whose expression is promoted by STAT1 and IFIH1 and inhibited by IRF1 and USP18, according to our regulatory network. To validate these findings, we measured CXCL10 secretion in STAT1-, IFIH1-, IRF1-, and USP18-silenced EC. Results demonstrated that stimulation of EC with IFN-α increased by 2-fold the secretion of CXCL10 protein. STAT1 silencing abrogated

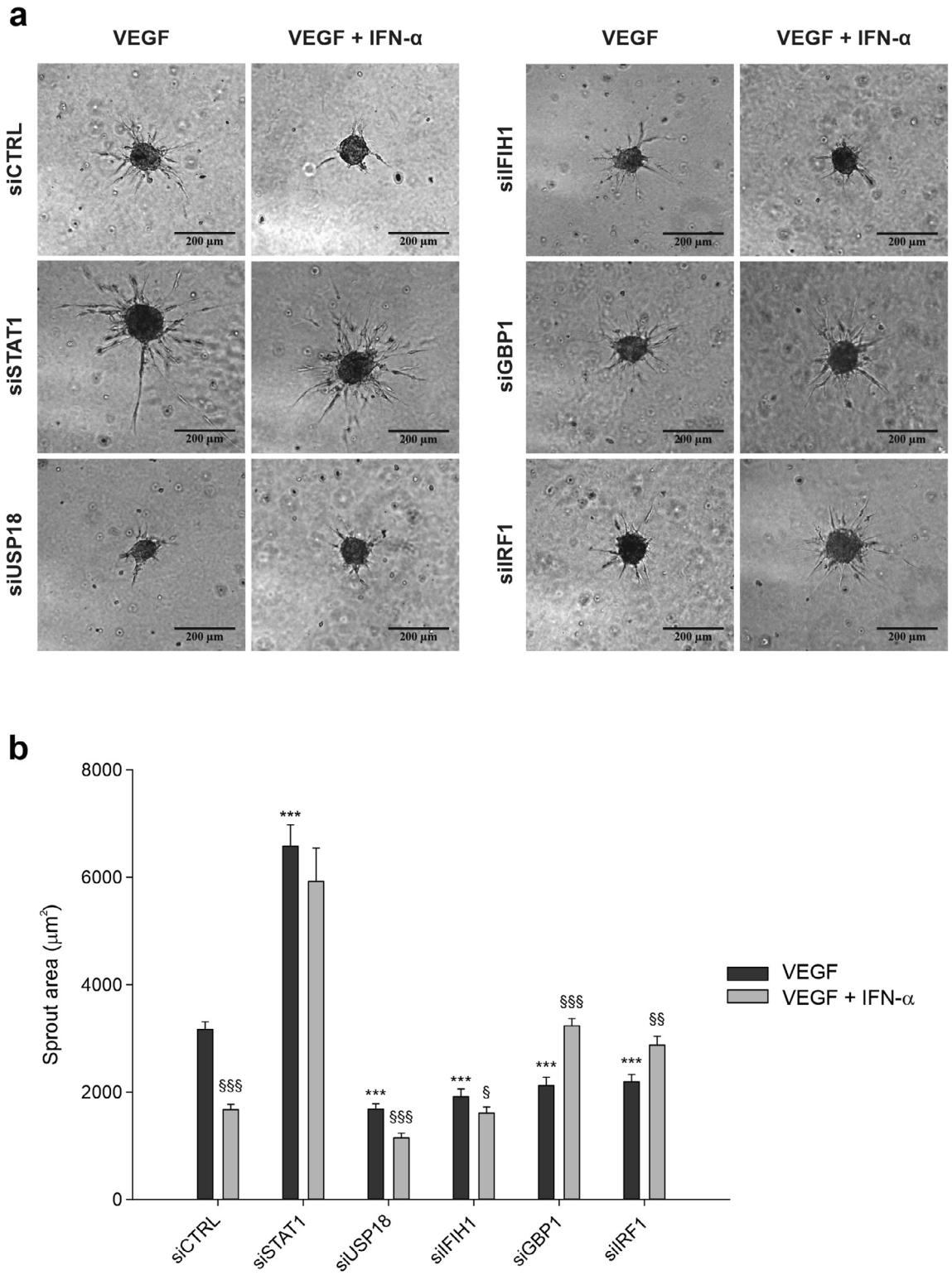

Fig. 4. Modulation of STAT1, USP18, IFIH1, GBP1, and IRF1 affects *in vitro* EC sprouting. (a) Representative pictures of spheroids obtained from 4 independent sprouting assays on HUVECs treated with 20 ng/ml VEGF, with or without 600 IU/ml IFN-α, upon STAT1, USP18, IFIH1, GBP1 and IRF1 silencing or scrambled siRNA treatment (siCTRL). (b) Quantification of sprout areas from 4 independent sprouting assays in the absence and in the presence of IFN-α. *** p<0.001 siSTAT1/USP18/IFIH1/GBP1/IRF1 vs. siCTRL; § p<0.05, §§ p<0.01, §§§ p<0.001 VEGF + IFN-α vs. VEGF alone.

IFN-α-induced upregulation of CXCL10, as expected. Silencing of USP18, on the contrary, strongly increased CXCL10 secretion, confirming an anticipated exacerbation of IFN-α signaling. Finally, the transcriptional effects induced by IFIH1 and IRF1 were not confirmed by this analysis. IFIH1 silencing produced only a mild reduction of CXCL10 secretion, while IRF1 silencing abrogated the effect of IFN-α on CXCL10. This last result is in line with the well-established positive role of IRF1 in the regulation of IFN-α pathway [32]. To assess whether STAT1, IFIH1, IRF1 and USP18 could have a role in the antiangiogenic activity of IFN-α, we per-

formed *in vitro* sprouting assay. We included in this analysis also GBP1, due to its established role in the inhibition of angiogenesis [45–47]. Treatment with IFN-α reduced by about 2-fold the number and the length of sprouts from EC spheroids, confirming the antiangiogenic activity of this cytokine. Consistent with the findings of Hsu and colleagues [48], which demonstrated that PML-induced isgylation of STAT1 has a critical role in the antiangiogenic activity of IFN-α and that USP18 has a proangiogenic role by deconjugating ISG15, we demonstrated that STAT1 knock-down abrogated, while USP18 silencing exacerbated, IFN-α-mediated inhibition of angiogenesis. Strikingly, knock-down of STAT1 doubled the generation of new sprouts even in the absence of IFN-α. This result suggests that angiogenesis could be physiologically inhibited by a tonic IFN-α signaling in EC, in part mediated by STAT1. To assess this hypothesis, we measured IFN-α secretion in 5 different pools of EC. Strikingly, we found that untransfected HUVECs secrete low amounts of endogenous IFN-α. Moreover, IFN-α signaling pathway is active in these cells, as demonstrated by the slight phosphorylation of STAT1, which is inhibited by the JAK inhibitor ruxolitinib. These results indicate that an autocrine signaling loop is physiologically active in EC, which secrete IFN-α, thus sustaining JAK/STAT signaling pathway and consequent synthesis of IFN-α. It should not be excluded, however, that other ligands contained in the complete cell culture medium, such as epidermal growth factor (EGF), could activate JAK/STAT signaling pathway in EC. The autocrine regulation of EC physiology could play an important role during tumorigenesis. In this scenario, tonic IFN-α signaling-mediated inhibition of angiogenesis is perturbed by the high levels of VEGF in the tumor microenvironment, which blunts IFN-α autocrine loop in EC through the degradation of IFNAR1 [26]. Consistently, our results demonstrated that STAT1 silencing not only abrogated the antiangiogenic activity of IFN-α, but strongly potentiated VEGF-mediated angiogenesis. In line with the putative regulation of angiogenesis by tonic IFN-α signaling, USP18 knock-down abrogated the proangiogenic activity of VEGF even in the absence of IFN-α. The same effect was observed by knocking-down IFIH1, GBP1 and IRF1, suggesting that these modulators restrict tonic IFN-α signaling and potentially regulate physiologic angiogenesis.

Overall, our findings could have therapeutic implications for cancer patients. Despite its potent anticancer activity, the use of IFN-α in the clinic was strongly limited by its severe side effects [49]. The pleiotropic activity of IFN-α on different tissues caused its replacement with targeted drugs, albeit often less potent. In this context, nanomedicine could redeem the clinical use of IFN-α by confining its activity in the tumor microenvironment. Nitric oxide-releasing nanoparticles are a viable strategy to exploit cancer metabolism to improve the enhanced permeability and retention (EPR) effect observed in solid tumors, thus promoting specific targeting of tumor tissues [50]. Loading such nanoparticles with IFN-α, along with a USP18-degrading proteolysis targeting chimera (PROTAC, a technology based on a chimeric molecule that specifically induces the ubiquitination and proteasome-mediated degradation of a target protein [51]), could increase IFN-α signaling in tumor vessels, overcoming proangiogenic stimuli released by cancer cells. Of note, cancer cells rapidly acquire several mechanisms of resistance to targeted drugs, such as bevacizumab [52], while the use of a pleiotropic cytokine, such as IFN-α, decreases the probability that a resistance mechanism could arise. The evidence that STAT1 blunts expression of VEGF-A in glioma cells [53] indicates that IFN-α suppresses angiogenesis by targeting both EC and cancer cells, suggesting that confining this cytokine in the tumor microenvironment and tuning its activity in EC could achieve a potent anticancer effect, while avoiding the marked side effects of systemic administration.

CRediT authorship contribution statement

Francesco Ciccarese: Conceptualization, Methodology, Validation, Investigation, Writing - original draft, Writing - review & editing, Visualization. **Angela Grassi:** Conceptualization, Methodology, Software, Formal analysis, Writing - original draft, Writing - review & editing, Visualization. **Lorenza Pasqualini:** Methodology, Validation, Investigation, Writing - original draft, Visualization. **Stefania Rosano:** Methodology, Validation, Investigation, Visualization. **Alessio Noghero:** Methodology, Validation, Investigation, Writing - original draft, Visualization. **Francesca Montenegro:** Methodology, Validation, Writing - review & editing, Investigation, Visualization. **Federico Bussolino:** Resources, Writing - original draft, Supervision. **Barbara Di Camillo:** Conceptualization, Methodology, Formal analysis. **Lorenzo Finesso:** Conceptualization, Funding acquisition. **Gianna Maria Toffolo:** Conceptualization, Methodology, Formal analysis, Supervision. **Stefania Mitola:** Resources. **Stefano Indraccolo:** Conceptualization, Methodology, Writing - original draft, Writing - review & editing, Resources, Supervision, Project administration, Funding acquisition.

Declaration of Competing Interest

The authors declare that they have no known competing financial interests or personal relationships that could have appeared to influence the work reported in this paper.

Acknowledgements

We thank Giampietro Viola (University of Padova) and Roberto Ronca (University of Brescia) for providing us with part of the endothelial cells used in this study. We thank Matteo Curtarello (Veneto Instituto of Oncology IOV-IRCCS) for help with initial qRT-PCR experiments. We thank Marco Falda (University of Padova) for help with graph visualization software. This work was supported by the Associazione Italiana per la Ricerca sul Cancro (Italian Association for Cancer Research) – IG 18803, by a grant of Regione Veneto (PRIL 2008-2010) and by a grant from Fondazione CARIPARO bando Progetti di Ricerca sul COVID-19.

Appendix A. Supplementary data

Supplementary data to this article can be found online at https://doi.org/10.1016/j.csbj.2020.11.048.

References

[1] Isaacs A, Baron S. Antiviral action of interferon in embryonic cells. The Lancet 1960;276:946–7. https://doi.org/10.1016/S0140-6736(60)92022-5.
[2] Samuel CE. Antiviral Actions of Interferons. Clin Microbiol Rev 2001;14:778–809.
[3] Tompkins WA. Immunomodulation and Therapeutic Effects of the Oral Use of Interferon-Alpha: Mechanism of Action. Journal of interferon & cytokine research: the official journal of the International Society for Interferon and Cytokine Research 1999, 19, doi:10.1089/107999099313325.
[4] Medrano RF, Hunger A, Mendonça SA, Barbuto JAM, Strauss BE. Immunomodulatory and antitumor effects of type I interferons and their application in cancer therapy. Oncotarget 2017;8:71249–84.
[5] Parker BS, Rautela J, Hertzog PJ. Antitumour actions of interferons: implications for cancer therapy. Nat Rev Cancer 2016;16:131–44. https://doi.org/10.1038/nrc.2016.14.
[6] Fuertes MB, Woo SR, Burnett B, Fu YX, Gajewski TF. Type I IFN response and innate immune sensing of cancer. Trends Immunol 2013;34:67–73. https://doi.org/10.1016/j.it.2012.10.004.
[7] Borden EC, Sen GC, Uze G, Silverman RH, Ransohoff RM, Foster GR, et al. Interferons at Age 50: Past, Current and Future Impact on Biomedicine. Nat Rev Drug Discovery 2007;6. https://doi.org/10.1038/nrd2422.
[8] Platanias L. Mechanisms of type-I- And type-II-interferon-mediated Signalling. *Nature reviews*. Immunology 2005;5. https://doi.org/10.1038/nri1604.
[9] Verma A, Deb D, Sassano A, Uddin S, Varga J, Wickrema A, et al. Activation of the p38 Mitogen-Activated Protein Kinase Mediates the Suppressive Effects of

Type I Interferons and Transforming Growth Factor-Beta on Normal Hematopoiesis. The Journal of biological chemistry 2002;277. https://doi.org/10.1074/jbc.M106640200.
[10] Schabbauer G, Luyendyk J, Crozat K, Jiang Z, Mackman N, Bahram S, et al. TLR4/CD14-mediated PI3K Activation Is an Essential Component of Interferon-Dependent VSV Resistance in Macrophages. Mol Immunol 2008;45. https://doi.org/10.1016/j.molimm.2008.02.001.
[11] Kaur S, Sassano A, Dolniak B, Joshi S, Majchrzak-Kita B, Baker D et al. Role of the Akt Pathway in mRNA Translation of Interferon-Stimulated Genes. Proceedings of the National Academy of Sciences of the United States of America 2008, 105, doi:10.1073/pnas.0710907105.
[12] Schreiber G, Piehler J. The Molecular Basis for Functional Plasticity in Type I Interferon Signaling. Trends Immunol 2015;36. https://doi.org/10.1016/j.it.2015.01.002.
[13] Indraccolo S. Interferon-alpha as Angiogenesis Inhibitor: Learning From Tumor Models. Autoimmunity 2010;43. https://doi.org/10.3109/08916930903510963.
[14] Raig E, Jones N, Varker K, Benniger K, Go M, Biber J et al. VEGF Secretion Is Inhibited by Interferon-Alpha in Several Melanoma Cell Lines. Journal of interferon & cytokine research: the official journal of the International Society for Interferon and Cytokine Research 2008, 28, doi:10.1089/jir.2008.0118.
[15] Oliveira I, Mukaida N, Matsushima K, Vilcek J. Transcriptional Inhibition of the interleukin-8 Gene by Interferon Is Mediated by the NF-kappa B Site. Molecular and cellular biology 1994, 14, doi:10.1128/mcb.14.8.5300.
[16] Padovan E, Spagnoli G, Ferrantini M, Heberer M. IFN-alpha2a Induces IP-10/CXCL10 and MIG/CXCL9 Production in Monocyte-Derived Dendritic Cells and Enhances Their Capacity to Attract and Stimulate CD8+ Effector T Cells. J Leukoc Biol 2002;71.
[17] Antonelli A, Ferrari S, Fallahi P, Ghiri E, Crescioli C, Romagnani P, et al. Beta and -Gamma Induce CXCL9 and CXCL10 Secretion by Human Thyrocytes: Modulation by Peroxisome Proliferator-Activated Receptor-Gamma Agonists. Cytokine 2010;50. https://doi.org/10.1016/j.cyto.2010.01.009.
[18] Persano L, Moserle L, Esposito G, Bronte V, Barbieri V, Iafrate M, et al. Interferon-alpha Counteracts the Angiogenic Switch and Reduces Tumor Cell Proliferation in a Spontaneous Model of Prostatic Cancer. Carcinogenesis 2009;30. https://doi.org/10.1093/carcin/bgp052.
[19] Liu P, Zhang C, Chen J, Zhang R, Ren J, Huang Yet al. Combinational Therapy of Interferon-α and Chemotherapy Normalizes Tumor Vasculature by Regulating Pericytes Including the Novel Marker RGS5 in Melanoma. Journal of immunotherapy (Hagerstown, Md. : 1997) 2011, 34, doi:10.1097/CJI.0b013e318213cd12.
[20] Marchisone C, Benelli R, Albini A, Santi L, Noonan D. Inhibition of Angiogenesis by Type I Interferons in Models of Kaposi's Sarcoma. Int J Biol Markers 1999;14.
[21] Wada H, Nagano H, Yamamoto H, Noda T, Murakami M, Kobayashi S, et al. Combination of Interferon-Alpha and 5-fluorouracil Inhibits Endothelial Cell Growth Directly and by Regulation of Angiogenic Factors Released by Tumor Cells. BMC cancer 2009;9. https://doi.org/10.1186/1471-2407-9-361.
[22] Indraccolo S, Pfeffer U, Minuzzo S, Esposito G, Roni V, Mandruzzato, S, et al. Identification of Genes Selectively Regulated by IFNs in Endothelial Cells. Journal of immunology (Baltimore, Md. : 1950) 2007, 178, doi:10.4049/jimmunol.178.2.1122.
[23] Pammer J, Reinisch C, Birner P, Pogoda K, Sturzl M, Tschachler E. Interferon-alpha Prevents Apoptosis of Endothelial Cells After Short-Term Exposure but Induces Replicative Senescence After Continuous Stimulation. Laboratory Investigation; A Journal of Technical Methods and Pathology 2006;86. https://doi.org/10.1038/labinvest.3700461.
[24] Brinckmann A, Axer S, Jakschies D, Dallmann I, Grosse J, Patzelt T, et al. Interferon-alpha Resistance in Renal Carcinoma Cells Is Associated With Defective Induction of Signal Transducer and Activator of Transcription 1 Which Can Be Restored by a Supernatant of Phorbol 12-myristate 13-acetate Stimulated Peripheral Blood Mononuclear Cells. Br J Cancer 2002;86. https://doi.org/10.1038/sj.bjc.6600066.
[25] Romero-Weaver A, Wang H, Steen H, Scarzello A, Hall V, Sheikh F, et al. Resistance to IFN-alpha-induced Apoptosis Is Linked to a Loss of STAT2. Molecular Cancer Research: MCR 2010;8. https://doi.org/10.1158/1541-7786.MCR-08-0344.
[26] Zheng H, Qian J, Carbone C, Leu N, Baker D, Fuchs S. Vascular Endothelial Growth Factor-Induced Elimination of the Type 1 Interferon Receptor Is Required for Efficient Angiogenesis. Blood 2011;118. https://doi.org/10.1182/blood-2011-06-359745.
[27] Gomez D, Reich N. Stimulation of Primary Human Endothelial Cell Proliferation by IFN. Journal of immunology (Baltimore, Md. : 1950) 2003, 170, doi:10.4049/jimmunol.170.11.5373.
[28] Reynolds J, Ray D, Zeef L, O'Neill T, Bruce I, Alexander M. The Effect of Type 1 IFN on Human Aortic Endothelial Cell Function in Vitro: Relevance to Systemic Lupus Erythematosus. Journal of interferon & cytokine research: the official journal of the International Society for Interferon and Cytokine Research 2014, 34, doi:10.1089/jir.2013.0016.
[29] Grassi A, Di Camillo B, Ciccarese F, Agnusdei V, Zanovello P, Amadori A, et al. Reconstruction of Gene Regulatory Modules From RNA Silencing of IFN-α Modulators: Experimental Set-Up and Inference Method. BMC Genomics 2016;17. https://doi.org/10.1186/s12864-016-2525-5.
[30] Rosano S, Corà D, Parab S, Zaffuto S, Isella C, Porporato R, et al. A Regulatory microRNA Network Controls Endothelial Cell Phenotypic Switch During Sprouting Angiogenesis. eLife 2020;9. https://doi.org/10.7554/eLife.48095.
[31] Zheng Y, Zheng X, Li S, Zhang H, Liu M, Yang Q, et al. Identification of Key Genes and Pathways in Regulating Immune-induced Diseases of Dendritic Cells by Bioinformatic Analysis. Mol Med Rep 2018;17. https://doi.org/10.3892/mmr.2018.8834.
[32] Honda K, Takaoka A, Taniguchi T. Type I Interferon Gene Induction by the Interferon Regulatory Factor Family of Transcription Factors. Immunity 2006;25. https://doi.org/10.1016/j.immuni.2006.08.009.
[33] Cheon, H.; Stark, G. Unphosphorylated STAT1 Prolongs the Expression of Interferon-Induced Immune Regulatory Genes. Proceedings of the National Academy of Sciences of the United States of America 2009, 106, doi:10.1073/pnas.0903487106.
[34] Santin I, Moore F, Grieco F, Marchetti P, Brancolini C, Eizirik D. USP18 is a key regulator of the interferon-driven gene network modulating pancreatic beta cell inflammation and apoptosis. Cell Death Dis 2012;3. https://doi.org/10.1038/cddis.2012.158.
[35] Korff T, Augustin HG. Integration of Endothelial Cells in Multicellular Spheroids Prevents Apoptosis and Induces Differentiation. J Cell Biol 1998;143:1341–52.
[36] Mostafavi S, Yoshida H, Moodley D, LeBoité H, Rothamel K, Raj T, et al. Parsing the Interferon Transcriptional Network and Its Disease Associations. Cell 2016;164. https://doi.org/10.1016/j.cell.2015.12.032.
[37] Malakhov M, Malakhova O, Kim K, Ritchie K, Zhang D. UBP43 (USP18) Specifically Removes ISG15 From Conjugated Proteins. The Journal of biological chemistry 2002;277. https://doi.org/10.1074/jbc.M109078200.
[38] Li L, Lei Q, Zhang S, Kong L, Qin B. Suppression of USP18 Potentiates the Anti-HBV Activity of Interferon Alpha in HepG2.2.15 Cells via JAK/STAT Signaling. PLoS ONE 2016;11. https://doi.org/10.1371/journal.pone.0156496.
[39] Wu B, Peisley A, Richards C, Yao H, Zeng X, Lin C, et al. Structural Basis for dsRNA Recognition, Filament Formation, and Antiviral Signal Activation by MDA5. Cell 2013;152. https://doi.org/10.1016/j.cell.2012.11.048.
[40] Brisse M, Ly H. Comparative Structure and Function Analysis of the RIG-I-Like Receptors: RIG-I and MDA5. Front Immunol 2019;10. https://doi.org/10.3389/fimmu.2019.01586.
[41] Liu S, Wang H, Jin Y, Podolsky R, Reddy M, Pedersen J, et al. IFIH1 Polymorphisms Are Significantly Associated With Type 1 Diabetes and IFIH1 Gene Expression in Peripheral Blood Mononuclear Cells. Hum Mol Genet 2009;18. https://doi.org/10.1093/hmg/ddn342.
[42] Honkala A, Tailor D, Malhotra S. Guanylate-Binding Protein 1: An Emerging Target in Inflammation and Cancer. Front Immunol 2020;10. https://doi.org/10.3389/fimmu.2019.03139.
[43] Forster, F.; Paster, W.; Supper, V.; Schatzlmaier, P.; Sunzenauer, S.; Ostler, N.; Saliba, A.; Eckerstorfer, P.; Britzen-Laurent, N.; Schütz, G., et al. Guanylate Binding Protein 1-mediated Interaction of T Cell Antigen Receptor Signaling With the Cytoskeleton. Journal of immunology (Baltimore, Md. : 1950) 2014, 192, doi:10.4049/jimmunol.1300377.
[44] Strieter R, Burdick M, Gomperts B, Belperio J, Keane M. CXC Chemokines in Angiogenesis. Cytokine Growth Factor Rev 2005;16. https://doi.org/10.1016/j.cytogfr.2005.04.007.
[45] Guenzi E, Töpolt K, Lubeseder-Martellato C, Jörg A, Naschberger E, Benelli R, et al. The Guanylate Binding protein-1 GTPase Controls the Invasive and Angiogenic Capability of Endothelial Cells Through Inhibition of MMP-1 Expression. The EMBO Journal 2003;22. https://doi.org/10.1093/emboj/cdg382.
[46] Weinländer K, Naschberger E, Lehmann M, Tripal P, Paster W, Stockinger H. Guanylate Binding protein-1 Inhibits Spreading and Migration of Endothelial Cells Through Induction of Integrin alpha4 Expression. FASEB journal: official publication of the Federation of American Societies for Experimental Biology 2008;22. https://doi.org/10.1096/fj.08-107524.
[47] Guenzi E, Töpolt K, Cornali E, Lubeseder-Martellato C, Jörg A, Matzen K, et al. The Helical Domain of GBP-1 Mediates the Inhibition of Endothelial Cell Proliferation by Inflammatory Cytokines. The EMBO journal 2001;20. https://doi.org/10.1093/emboj/20.20.5568.
[48] Hsu KS, Zhao X, Cheng X, Guan D, Mahabeleshwar GH, Liu Y, et al. Dual regulation of Stat1 and Stat3 by the tumor suppressor protein PML contributes to interferon α-mediated inhibition of angiogenesis. J Biol Chem 2017;292:10048–60. https://doi.org/10.1074/jbc.M116.771071.
[49] Hepgul N, Cattaneo A, Agarwal K, Baraldi S, Borsini A, Bufalino C, et al. Transcriptomics in Interferon-α-Treated Patients Identifies Inflammation-, Neuroplasticity- And Oxidative Stress-Related Signatures as Predictors and Correlates of Depression. *Neuropsychopharmacology : official publication of the American College of.* Neuropsychopharmacology 2016;41. https://doi.org/10.1038/npp.2016.50.
[50] Ciccarese F, Raimondi V, Sharova E, Silic-Benussi M, Ciminale V. Nanoparticles as Tools to Target Redox Homeostasis in Cancer Cells. Antioxidants (Basel, Switzerland) 2020;9. https://doi.org/10.3390/antiox9030211.
[51] Sun X, Gao H, Yang Y, He M, Wu Y, Song Y, et al. PROTACs: great opportunities for academia and industry. Signal Transduct Target Ther 2019;4:64. https://doi.org/10.1038/s41392-019-0101-6.
[52] Zarrin B, Zarifi F, Vaseghi G, Javanmard SH. Acquired tumor resistance to antiangiogenic therapy: Mechanisms at a glance. In J Res Med Sci 2017;22.
[53] Zhang Y, Jin G, Zhang J, Mi R, Zhou Y, Fan W, et al. Overexpression of STAT1 Suppresses Angiogenesis Under Hypoxia by Regulating VEGF-A in Human Glioma Cells. Biomedicine & pharmacotherapy = Biomedecine & pharmacotherapie 2018;104. https://doi.org/10.1016/j.biopha.2018.05.079.